

# ***BUCKLING OF PLAIN MASONRY WALLS WITH INITIAL DOUBLE CURVATURE***

by

M. Hatzinikolas, J. Longworth, and J. Warwaruk

**ALBERTA  
MASONRY  
INSTITUTE**



# BUCKLING OF PLAIN MASONRY WALLS WITH INITIAL DOUBLE CURVATURE

By Hatzinikolas, M., Longworth, J., and Warwaruk, J.

**ABSTRACT:** Masonry walls loaded in double curvature tend to fail in the first buckling mode. The buckling loads for masonry walls with initial double curvature imperfections or moments are evaluated using the energy approach and fifth order polynomials for interpolating functions. Results for a number of full scale walls tested under double curvature moments are compared with the analytical results.

The method for the evaluation of the buckling load for masonry walls with initial double curvature imperfections or moments is presented. The method is based on the energy approach and fifth order polynomials for interpolating functions. The results for a number of full scale walls tested under double curvature moments are compared with the analytical results. The method is based on the energy approach and fifth order polynomials for interpolating functions. The results for a number of full scale walls tested under double curvature moments are compared with the analytical results.

## BUCKLING OF MASONRY WALLS

Solutions to the buckling problem of walls of columns without lateral supports were proposed by Chapman, J.O. and Stafford, J.P. (1) and by Yeh, F.K. (2). The solution of the differential equations presented in Reference (1) for walls with initial double curvature bending gives the following expression for the critical load:

$$P_{cr} = \frac{0.285 \frac{EI}{L^2} (0.5t - e)^2}{1 + \frac{e^2}{L^2}}$$

where  $E$  = the modulus of elasticity of the masonry  
 $t$  = thickness of the wall  
 $e$  = eccentricity of the applied load  
 $L$  = the length of the wall  
 $I$  = uncracked moment of inertia

This solution can be approximated with an accuracy of 2.5% by

$$P_{cr} = 8\pi^2 \frac{EI}{L^2} (0.5 - \frac{e}{t})^2$$

Graduate Student, The University of Alberta, Edmonton, Canada  
 Professor of Civil Engineering, University of Alberta, Edmonton, Canada T6N 2G7  
 Professor of Civil Engineering, University of Alberta, Edmonton, Canada T6N 2G7



# BUCKLING OF PLAIN MASONRY WALLS WITH INITIAL DOUBLE CURVATURE

By M. Hatzinikolas<sup>1</sup>, J. Longworth<sup>2</sup>, J. Warwaruk<sup>3</sup>

## INTRODUCTION

Recently a number of researchers have studied the application of the moment magnifier method to the design of load bearing masonry walls. The method has been shown to give satisfactory results for walls bent in single curvature and for eccentricities within the kern. Most significant is the work of Dikkers, R.D. and Yokel, F.Y.<sup>(1)</sup> and that of Faltal, S.G. and Cattaneo, L.E.<sup>(2)</sup>. For walls subjected to double curvature bending it is assumed that the moment magnifier method will give satisfactory results because of the increased buckling load. In this paper a method of evaluating the critical load for masonry walls with initial double curvature bending is presented and test results for a number of full scale specimens are reported.

## BUCKLING OF MASONRY WALLS

Solutions to the buckling problem of walls or columns without tensile strength were proposed by Chapman, J.C. and Slafford, J.<sup>(3)</sup> and by Yokel, F.Y.<sup>(4)</sup>. The solution of the differential equations presented in Reference (4) for walls in single curvature bending gives the following expression for the critical load:

$$P_{cr} = 0.285 \frac{9}{4} \pi^2 \frac{(0.5t - e)^3 EI_o}{L^2} \quad [1]$$

where E = the modulus of elasticity of the masonry  
t = thickness of the wall  
e = eccentricity of the applied load  
L = the length of the wall.  
I<sub>o</sub> = uncracked moment of inertia.

This solution can be approximated with an accuracy of 3.8% by

$$P_{cr} = 8\pi^2 \left(0.5 - \frac{e}{t}\right)^3 \frac{EI_o}{L^2} \quad [2]$$

---

<sup>1</sup> Graduate Student, The University of Alberta, Edmonton, Canada  
T6G 2G7

<sup>2</sup> Professor of Civil Engineering, University of Alberta, Edmonton,  
Canada T6G 2G7

<sup>3</sup> Professor of Civil Engineering, University of Alberta, Edmonton,  
Canada T6G 2G7

The first buckling mode is a lower energy configuration than the second mode, and as a result of this, regardless of the loading condition and initial imperfection, the member tends to assume this configuration. When this happens, the cracks created by the end moments on one side of the wall will close and, in effect, this side will be uncracked. The member may then be analyzed as a "stepped-column" as shown in Figure 1.

Initially the location of the point of inflection is given by

$$\alpha = \frac{e_1}{e_1 + e_2}$$

where  $e_1$  = the smaller of the two end eccentricities  
 $e_2$  = the larger of the two end eccentricities

The moment of inertia of the cracked section may be approximated on the basis of Equation 2 as:

$$I_1 = 8(0.5 - \frac{e_2}{t})^3 I_0$$

and the section can be now analyzed as the column shown in Figure 2.

#### EVALUATION OF BUCKLING LOAD OF EQUIVALENT SECTION BY THE ENERGY METHOD

The total potential energy at buckling for any member subjected to combined bending and axial load is given by

$$\Pi_B = 1/2 \int_0^L EI_0 (y'')^2 dx - 1/2 P_{cr} \int_0^L (y')^2 dx \quad [3]$$

where  $y$  = the buckled shape.

For an elastic structure the total potential  $\Pi_B$  is composed of the strain energy and the potential of the applied load. The equilibrium condition is expressed mathematically as:

$$\delta \Pi_B = 0$$

[4]

To solve the buckling load for the stepped column an appropriate buckled shape is selected and the condition of Equation 4 is imposed on the total potential relation.

To obtain the best possible shape for the buckling configuration, a finite element approach is used with a fifth order interpolating function.

Equation 3 is rewritten to account for the different section properties in the two segments as follows:

$$\Pi_B = 1/2 \int_0^{\alpha L} EI_0 (y''')^2 + 1/2 \int_{\alpha L}^L EI (y''')^2 dx - 1/2 P_{cr} \int_0^L (y')^2 dx \quad [5]$$

Letting  $y = \langle \phi \rangle \{ \theta \}$

Then

$$y' = \langle \phi' \rangle \{ \theta \}$$

$$y''' = \langle \phi''' \rangle \{ \theta \}$$

$$(y')^2 = \langle \phi' \rangle \{ \theta \} \langle \phi' \rangle \{ \theta \} = \{ \theta \} [\phi'] \{ \theta \}$$

$$(y''')^2 = \langle \phi''' \rangle \{ \theta \} \langle \phi''' \rangle \{ \theta \} = \{ \theta \} [\phi'''] \{ \theta \}$$

where

$y$  = deflection

$y'$  = slope

$y'''$  = curvature

$\langle \phi \rangle = \langle \phi_1 \phi_2 \phi_3 \phi_4 \phi_5 \phi_6 \rangle$ , the interpolating functions,

and

$$\{ \theta \} = \begin{bmatrix} y_1 \\ y_1' \\ y_1'' \\ y_2 \\ y_2' \\ y_2'' \end{bmatrix}$$

Since end deflections  $y_1$  and  $y_2$  are zero, the interpolating functions  $\phi_1$  and  $\phi_4$  must be zero.

Changing the limits of integration and substituting for  $y'''$  and  $y'$  in Equation 5, the following relation is obtained for the total potential

$$\Pi_B = 1/2 \frac{EI_0}{L} \int_0^{\alpha} \{ \theta \} [\phi'''] \{ \theta \} dn + 1/2 \frac{EI_1}{L} \int_{\alpha}^1 \{ \theta \} [\phi'''] \{ \theta \} dn - 1/2 P_{cr} L \int_0^1 \{ \theta \} [\phi'] \{ \theta \} dn$$

Applying Equation 4 to the above, the equilibrium condition may be expressed as

$$\delta \Pi_B = \frac{EI}{L} \int_0^{\alpha} [\phi'''] \{ \theta \} dn + \frac{EI_1}{L} \int_{\alpha}^1 [\phi'''] \{ \theta \} dn - P_{cr} L \int_0^1 [\phi'] \{ \theta \} dn = 0$$



$$\text{or, } \int_0^\alpha [\phi'''] \{\theta\} \, dn + \beta \int_\alpha^1 [\phi'''] \{\theta\} \, dn = \frac{P_{cr} L^2}{EI_0} \int_0^1 [\phi'] \{\theta\} \, dn$$

$$\text{where } \beta = \frac{I_1}{I_0}$$

The above relation can be reduced to

$$[K] \{\theta\} = \lambda [K_g] \{\theta\} \quad [6]$$

where  $[K]$  = bending stiffness matrix  
 $[K_g]$  = geometric stiffness matrix

This equation is solved as an Eigen value problem to find  $\lambda$ .

For  $L^2/EI_0 = 1$  the above relation can be solved to obtain the coefficients which will give the buckling load  $P_{cr} = \lambda EI_0/L^2$  for values of  $\alpha$  and  $\beta$ . Table 1 is a tabulation of  $\lambda$  values as found using this method. The interpolating functions and the boundary conditions used are given in the Appendix. Table 1 can be used to evaluate  $P_{cr}$  for any stepped column of constant modulus of elasticity by entering with  $\alpha$  and  $\beta$  finding  $\lambda$  and multiplying  $\lambda$  by  $EI_0/L^2$ .

The advantages of using this method are:

- (a) High order polynomials will approximate very closely a sine curve and other shapes that a stepped column can assume as a result of initial bending and variations in the geometric properties. It is found that a fifth order polynomial is quite adequate in this case.
- (b) Using a determinant search method and approaching the solution from the left will assure the selection of the best shape to minimize the energy stored in the system.

#### EXPERIMENTAL PROGRAM AND RESULTS

Ten plain walls were built using 8x8x16 two core C-90 blocks and type S mortar. The end eccentricities and the slenderness ratios of the walls tested are listed in Table 2.

The walls were tested in a 1.6 million pound capacity testing machine at ages varying from 28 to 65 days. Deflections were monitored throughout each test and the deflected shapes at selected loads were plotted. The tendency of the walls to fail in their first buckling modes is shown in Figure 4 and 5. Figure 6 shows the calculated and experimental buckling loads. The theoretical analysis was based on  $I_0 = 1200 \text{ in.}^4$  and  $E = 1.35 \times 10^6 \text{ psi}$ . Table 2 gives a summary of test results. As expected, the experimental results were lower than the theoretical buckling loads because material failures occurred before the buckling loads were reached. This type of failure is more probable than buckling failure for small eccentricities and slenderness ratios less than 30. However the mode of failure was in close agreement with the

assumed first mode. Movement of the point of inflection with increasing load was observed, which further strengthens the assumption that the first buckling mode is the more critical, regardless of the end conditions. Figure 5 shows a comparison of test results with theoretical values.

## CONCLUSIONS

Masonry walls subjected to double curvature bending tend to buckle in their first buckling mode. The critical loads for such walls can be obtained using energy methods and fifth order polynomials for interpolation functions. The results, using one element and fifth order interpolating functions, are good estimates of the buckling loads. For a wall with a constant moment of inertia, the error is 0.048%. The coefficients for evaluating the critical loads for walls subjected to double curvature bending can be used in the moment magnifier method in designing such walls.

## ACKNOWLEDGEMENTS

This study was performed in the Department of Civil Engineering at the University of Alberta. Financial assistance from the Canadian Masonry Institute, the Alberta Masonry Institute and the National Research Council of Canada is acknowledged.

## REFERENCES

1. Dikkers, R.D. and Yokel, F.Y., "Strength of Brick Wall Subject to Axial Compression and Bending", Proceedings of Second International Brick Masonry Conference held in Stoke-on-Trent, England, April 1970.
2. Fattal, S.G. and Cattaneo, L.E., "Structural Performance of Masonry Wall Under Compression and Flexure", U.S. Department of Commerce, National Bureau of Standards, Ernest Ambler, Acting Director, Issued June 1976.
3. Chapman, J.C. and Slafford, J., "The Elastic Buckling of Brittle Columns", Par No. 6147, Proceedings of the Institution of Civil Engineers, London, Volume 6, pp. 107-125, January 1957.
4. Yokel, F.Y., "Stability and Load Capacity of Member with No Tensile Strength", Journal of the Structural Division, Proceedings of the American Society of Civil Engineers, July 1971.



## APPENDIX

### EVALUATION OF INTERPOLATING FUNCTION

All mathematical operations involving interpolating functions and the solution of the buckling problem were carried out using a computer.

Since deflections are zero at both ends  $\phi_1$  and  $\phi_4$  are zero. The remaining four functions are shown schematically in Figure 3. The boundary conditions to be satisfied by these functions ( $\phi_2, \phi_3, \phi_5, \phi_6$ ) are as follows:

| $\eta$ | $y$ | $y'$ | $y''$ | functions |
|--------|-----|------|-------|-----------|
| 0      | 0   | 1    | 0     | $\phi_2$  |
| 1      | 0   | 0    | 0     |           |
| 0      | 0   | 0    | 1     | $\phi_3$  |
| 1      | 0   | 0    | 0     |           |
| 0      | 0   | 0    | 0     | $\phi_5$  |
| 1      | 0   | 1    | 0     |           |
| 0      | 0   | 0    | 0     | $\phi_6$  |
| 1      | 0   | 0    | 1     |           |

The functions which satisfy these conditions are:

$$\begin{aligned}\phi_2 &= -3\eta^8 + 8\eta^4 - 6\eta^3 + \eta \\ \phi_3 &= -1/2 (\eta^8 - 3\eta^4 + 3\eta^3 - \eta^2) \\ \phi_5 &= -3\eta^8 + 7\eta^4 - 4\eta^3 \\ \phi_6 &= 1/2 (\eta^8 - 2\eta^4 + \eta^3)\end{aligned}$$

Differentiating these functions once yields

$$[\Phi'] = \begin{bmatrix} \phi_2' & \phi_2' & \phi_2' & \phi_3' & \phi_2' & \phi_5' & \phi_2' & \phi_6' \\ & \phi_2' & \phi_3' & \phi_3' & \phi_5' & \phi_3' & \phi_6' \\ & & \phi_3' & \phi_5' & \phi_5' & \phi_6' \\ \text{symmetric} & & & \phi_5' & \phi_5' & \phi_6' \\ & & & & \phi_6' & \phi_6' \end{bmatrix}$$

Substitution of the functions and integration of the above matrix from 0 to 1 results in



$$\int_0^1 [\Phi'] \, dn = \begin{bmatrix} 0.22857 & 0.016666 & -0.014285 & 0.004762 \\ & 0.0015873 & -0.004762 & 0.000793 \\ \text{symmetric} & & 0.228571 & -0.016667 \\ & & & 0.001587 \end{bmatrix} = [K_g]$$

where  $[K_g]$  is the geometric stiffness matrix.

The interpolating functions are then differentiated twice and the matrix  $[\Phi'']$  is obtained as:

$$[\Phi''] = \begin{bmatrix} \phi_2'' & \phi_2'' & \phi_2'' & \phi_3'' & \phi_2'' & \phi_5'' & \phi_2'' & \phi_6'' \\ & \phi_3'' & \phi_3'' & \phi_3'' & \phi_5'' & \phi_3'' & \phi_6'' \\ \text{symmetric} & & \phi_5'' & \phi_5'' & \phi_5'' & \phi_6'' \\ & & & \phi_6'' & \phi_6'' \end{bmatrix}$$

After substitution of the corresponding functions, integrating this matrix and evaluating  $[\Phi'']_0^\alpha + C[\Phi'']_\alpha^1$ , the bending stiffness matrix,  $[K]$ , is obtained.

For the case of a column with constant  $EI_1$  ( $\alpha = 0$ ) this matrix is

$$[K] = \begin{bmatrix} 5.4857 & 0.3143 & +3.0857 & -0.11428 \\ & 0.0857 & 0.1143 & 0.01428 \\ \text{symmetric} & & 5.4857 & -0.31428 \\ & & & 0.00857 \end{bmatrix}$$

Solving the relation

$$[K] \{\theta\} = P_{cr} \frac{L^2}{EI_0} [K_g] \{\theta\}$$

$$\text{for } \frac{L^2}{EI_0} = 1$$

and the geometric and bending stiffness matrices,  $[K_g]$  and  $[K]$  as evaluated above, using the power sweep method,  $P_{cr} = 9.8734354$  which compares very closely with the exact value of  $\pi^2$ . Table 1 is obtained by evaluating  $[K]$  and solving relations for various values of  $\alpha$  and  $\beta$  from 0.0 to 1.

Table 1 - Buckling Coefficients for Stepped Walls and Columns

| $\beta \backslash \alpha$ | 0.0  | 0.05 | 0.10 | 0.15 | 0.20 | 0.25 | 0.30 | 0.35 | 0.40 | 0.45 | 0.50 | 0.55 | 0.60 | 0.65 | 0.70 | 0.75 | 0.80 | 0.85 | 0.90 | 0.95 | 1.00 |
|---------------------------|------|------|------|------|------|------|------|------|------|------|------|------|------|------|------|------|------|------|------|------|------|
| 0.05                      | 0.49 | 0.50 | 0.52 | 0.54 | 0.57 | 0.61 | 0.66 | 0.76 | 0.92 | 1.18 | 1.52 | 1.94 | 2.42 | 2.98 | 3.74 | 4.92 | 6.81 | 8.84 | 9.71 | 9.87 | 9.88 |
| 0.10                      | 0.99 | 0.99 | 1.02 | 1.06 | 1.11 | 1.18 | 1.26 | 1.33 | 1.58 | 1.89 | 2.35 | 2.95 | 3.67 | 4.50 | 5.47 | 6.63 | 7.99 | 9.17 | 9.74 | 9.87 | 9.88 |
| 0.15                      | 1.48 | 1.48 | 1.51 | 1.57 | 1.64 | 1.72 | 1.83 | 1.98 | 2.20 | 2.54 | 3.03 | 3.70 | 4.52 | 5.45 | 6.45 | 7.51 | 8.54 | 9.35 | 9.70 | 9.87 | 9.88 |
| 0.20                      | 1.98 | 1.98 | 2.01 | 2.07 | 2.18 | 2.26 | 2.39 | 2.55 | 2.79 | 3.15 | 3.66 | 4.34 | 5.17 | 6.11 | 7.08 | 8.02 | 8.85 | 9.46 | 9.78 | 9.87 | 9.88 |
| 0.25                      | 2.47 | 2.47 | 2.50 | 2.57 | 2.66 | 2.78 | 2.93 | 3.11 | 3.37 | 3.73 | 4.24 | 4.91 | 5.73 | 6.63 | 7.53 | 8.36 | 9.04 | 9.53 | 9.79 | 9.87 | 9.88 |
| 0.30                      | 2.98 | 2.97 | 2.99 | 3.06 | 3.18 | 3.29 | 3.45 | 3.65 | 3.92 | 4.28 | 4.78 | 5.43 | 6.20 | 7.05 | 7.88 | 8.81 | 9.18 | 9.59 | 9.80 | 9.87 | 9.88 |
| 0.35                      | 3.48 | 3.46 | 3.49 | 3.55 | 3.66 | 3.80 | 3.97 | 4.17 | 4.45 | 4.81 | 5.29 | 6.90 | 6.63 | 7.41 | 8.15 | 8.80 | 9.29 | 9.03 | 9.81 | 9.87 | 9.88 |
| 0.40                      | 3.95 | 3.95 | 3.98 | 4.04 | 4.15 | 4.29 | 4.47 | 4.68 | 4.95 | 5.31 | 5.77 | 6.35 | 7.02 | 7.72 | 8.39 | 8.95 | 9.36 | 9.66 | 9.82 | 9.87 | 9.88 |
| 0.45                      | 4.44 | 4.45 | 4.47 | 4.53 | 4.64 | 4.78 | 4.96 | 5.18 | 5.45 | 5.79 | 6.23 | 6.78 | 7.37 | 8.00 | 8.59 | 9.08 | 9.45 | 9.09 | 9.83 | 9.87 | 9.88 |
| 0.50                      | 4.94 | 4.94 | 4.96 | 5.02 | 5.12 | 5.27 | 5.44 | 5.66 | 5.92 | 6.25 | 6.66 | 7.14 | 7.69 | 8.25 | 8.76 | 9.19 | 9.51 | 9.72 | 9.88 | 9.87 | 9.88 |
| 0.55                      | 5.43 | 5.43 | 5.45 | 5.51 | 5.81 | 5.74 | 5.91 | 6.12 | 6.38 | 6.69 | 7.06 | 7.50 | 7.99 | 8.47 | 8.92 | 9.29 | 9.56 | 9.76 | 9.84 | 9.87 | 9.88 |
| 0.60                      | 5.93 | 5.93 | 5.95 | 6.00 | 6.09 | 6.22 | 6.38 | 6.58 | 6.82 | 7.10 | 7.44 | 7.84 | 8.26 | 8.68 | 9.06 | 9.38 | 9.61 | 9.76 | 9.84 | 9.87 | 9.88 |
| 0.65                      | 6.42 | 6.42 | 6.44 | 6.48 | 6.57 | 6.69 | 6.84 | 7.02 | 7.24 | 7.50 | 7.81 | 8.15 | 8.51 | 8.87 | 9.19 | 9.46 | 9.65 | 9.78 | 9.86 | 9.87 | 9.88 |
| 0.70                      | 6.91 | 6.91 | 6.93 | 6.97 | 7.04 | 7.15 | 7.29 | 7.46 | 7.65 | 7.89 | 8.15 | 8.44 | 8.75 | 9.05 | 9.31 | 9.53 | 9.89 | 9.80 | 9.85 | 9.87 | 9.88 |
| 0.75                      | 7.41 | 7.41 | 7.42 | 7.46 | 7.52 | 7.61 | 7.73 | 7.88 | 8.05 | 8.25 | 8.48 | 8.72 | 8.97 | 9.21 | 9.42 | 9.60 | 9.73 | 9.81 | 9.86 | 9.87 | 9.88 |
| 0.80                      | 7.90 | 7.90 | 7.91 | 7.94 | 7.99 | 8.07 | 8.17 | 8.30 | 8.44 | 8.60 | 8.79 | 8.98 | 9.17 | 9.36 | 9.53 | 9.66 | 9.78 | 9.83 | 9.86 | 9.87 | 9.88 |
| 0.85                      | 8.39 | 8.39 | 8.40 | 8.43 | 8.47 | 8.53 | 8.61 | 8.70 | 8.81 | 9.94 | 9.08 | 9.22 | 9.37 | 9.50 | 9.62 | 9.72 | 9.79 | 9.84 | 9.80 | 9.87 | 9.88 |
| 0.90                      | 8.89 | 8.89 | 8.89 | 8.91 | 8.94 | 8.98 | 9.03 | 9.10 | 9.16 | 9.26 | 9.36 | 9.45 | 9.55 | 9.63 | 9.71 | 9.77 | 9.82 | 9.82 | 9.87 | 9.87 | 9.88 |
| 0.95                      | 9.38 | 9.38 | 9.38 | 9.39 | 9.41 | 9.43 | 9.46 | 9.49 | 9.53 | 9.58 | 9.62 | 9.67 | 9.72 | 9.76 | 9.80 | 9.83 | 9.85 | 9.86 | 9.87 | 9.87 | 9.88 |
| 1.00                      | 9.88 | 9.88 | 9.88 | 9.88 | 9.88 | 9.88 | 9.88 | 9.88 | 9.88 | 9.88 | 9.88 | 9.88 | 9.88 | 9.88 | 9.88 | 9.88 | 9.88 | 9.88 | 9.88 | 9.88 | 9.88 |



Table 2 - Loading Conditions and Test Results

| Wall No. | h/t   | e <sub>1</sub><br>(inches) | e <sub>2</sub><br>(inches) | Load at failure<br>(kips) |
|----------|-------|----------------------------|----------------------------|---------------------------|
| E1       | 17.97 | +3.54                      | -3.54                      | 85.0                      |
| E2       | 15.87 | +3.54                      | -3.54                      | 115.0                     |
| E3       | 13.77 | +3.54                      | -3.54                      | 135.2                     |
| E4       | 13.77 | +2.54                      | -2.54                      | 156.6                     |
| E5       | 13.77 | +1.27                      | -1.27                      | 220.4                     |
| G5       | 17.97 | +2.54                      | -3.00                      | 150.6                     |
| G6       | 17.97 | +2.54                      | -3.54                      | 144.4                     |
| G7       | 17.97 | +1.27                      | -1.27                      | 196.6                     |
| G8       | 17.97 | +3.00                      | -3.54                      | 117.0                     |
| G9       | 17.97 | +3.00                      | -3.00                      | 148.2                     |
| M1       | 24.20 | 0.00                       | 0.00                       | 139.2                     |

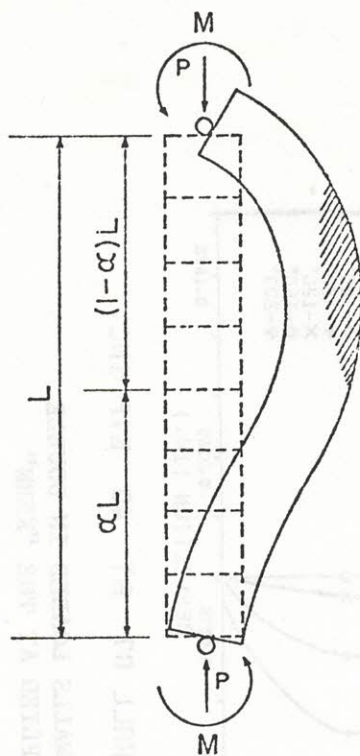


FIGURE 1: CRACKED SECTION AT BUCKLING UNDER THE ACTION OF AXIAL LOAD AND DOUBLE CURVATURE BENDING

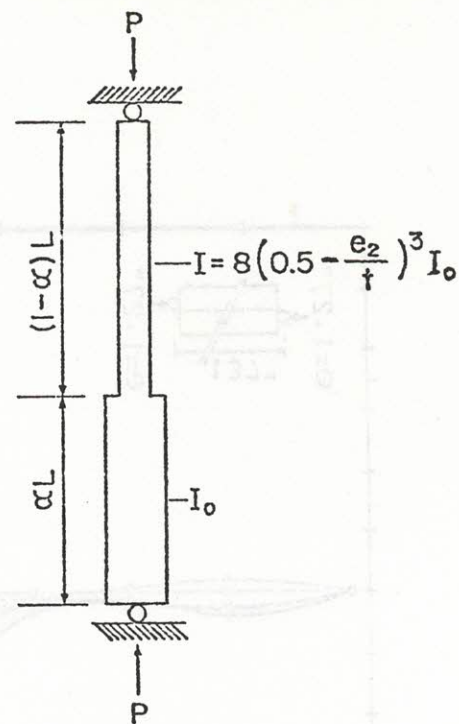


FIGURE 2: EQUIVALENT SECTION

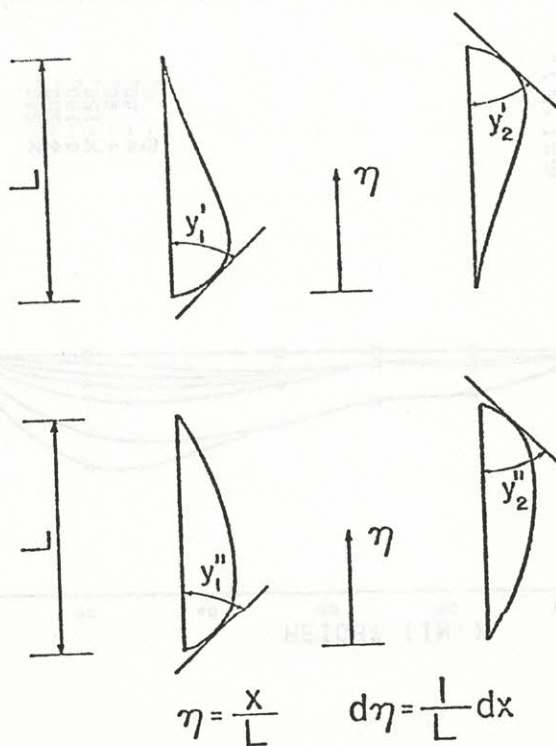
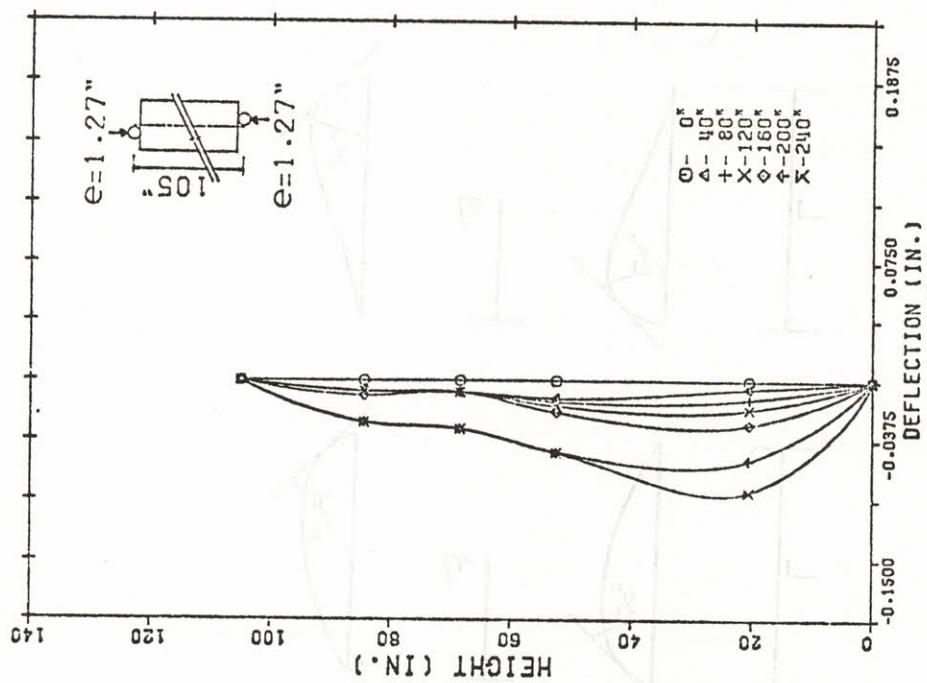
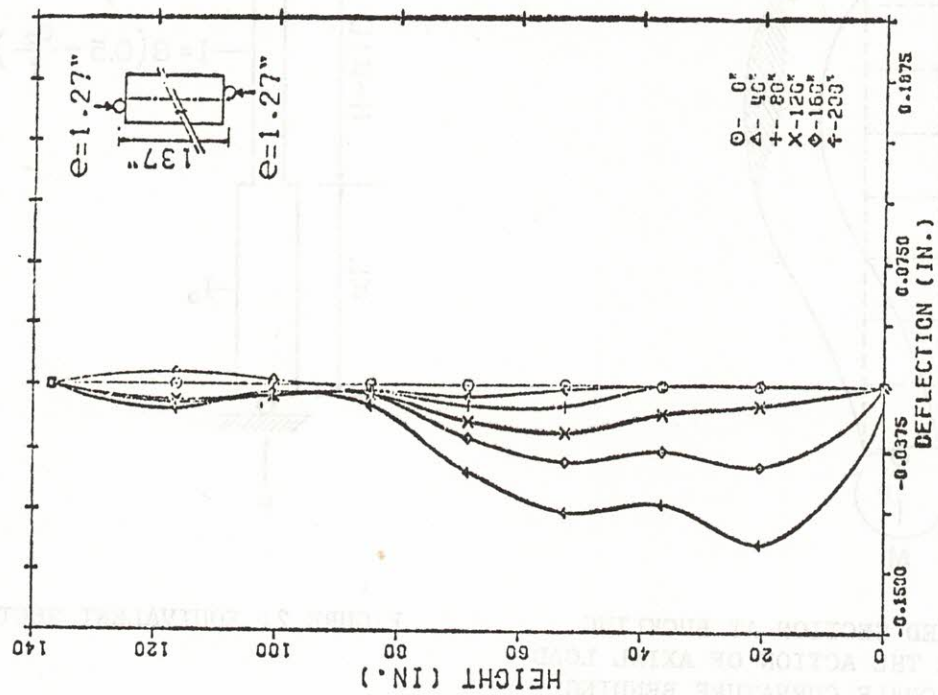


FIGURE 3: INTERPOLATING FUNCTIONS





WALL E5 AT 40 KIP INC.



WALL G7 AT 40 KIP INC.

FIGURE 4: LOAD DEFLECTION CURVES FOR WALLS LOADED IN DOUBLE CURVATURE WITH THE LOAD APPLIED AT THE "KERN" POINT.

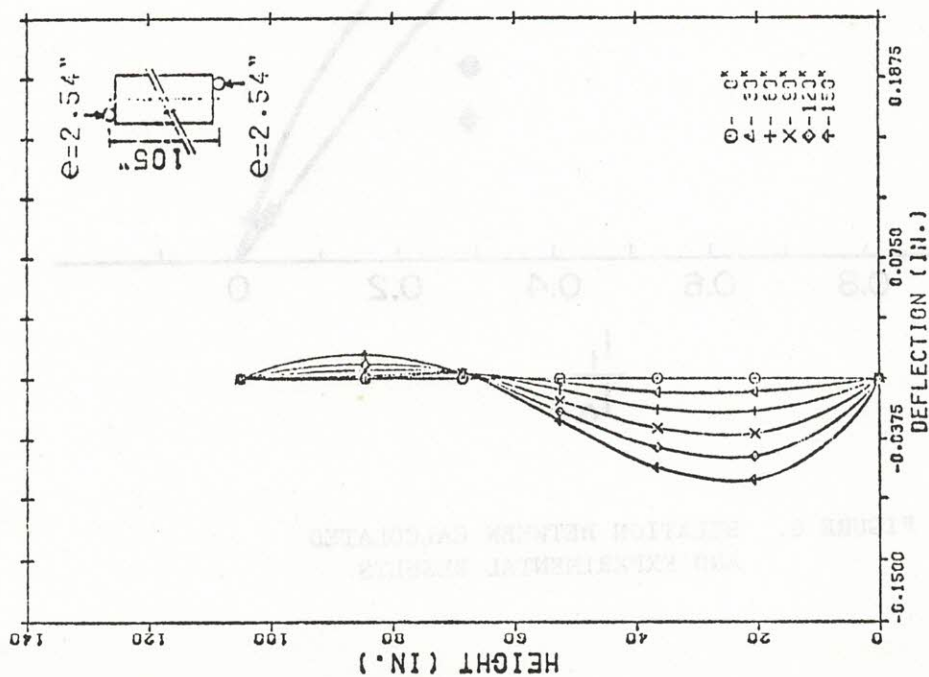
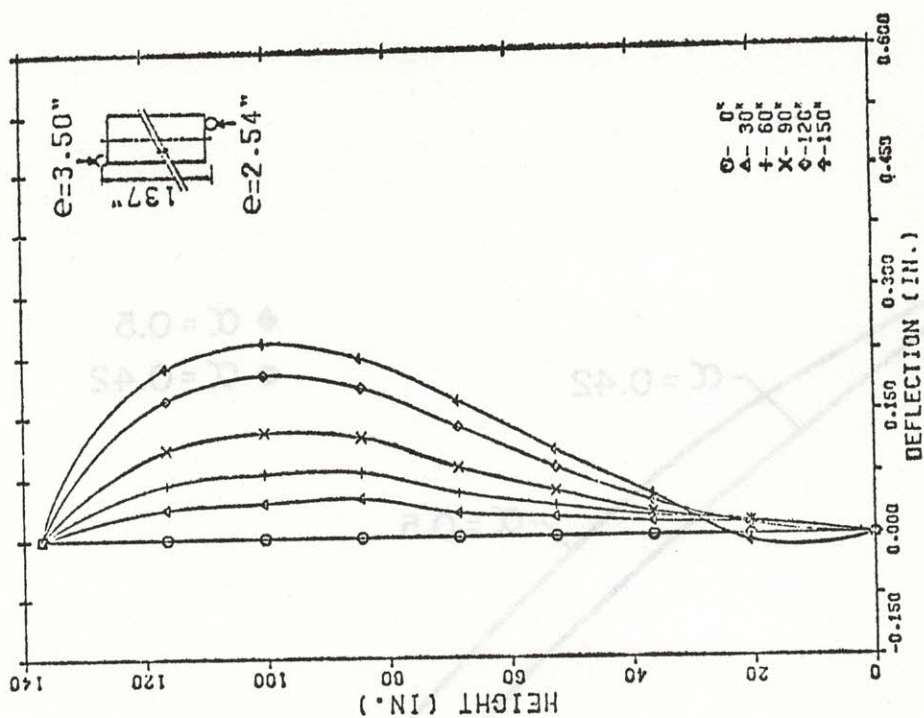


FIGURE 5: LOAD DEFLECTION CURVES FOR WALLS LOADED IN DOUBLE CURVATURE WITH ECCENTRICITY LARGER THAN THE "KERN".



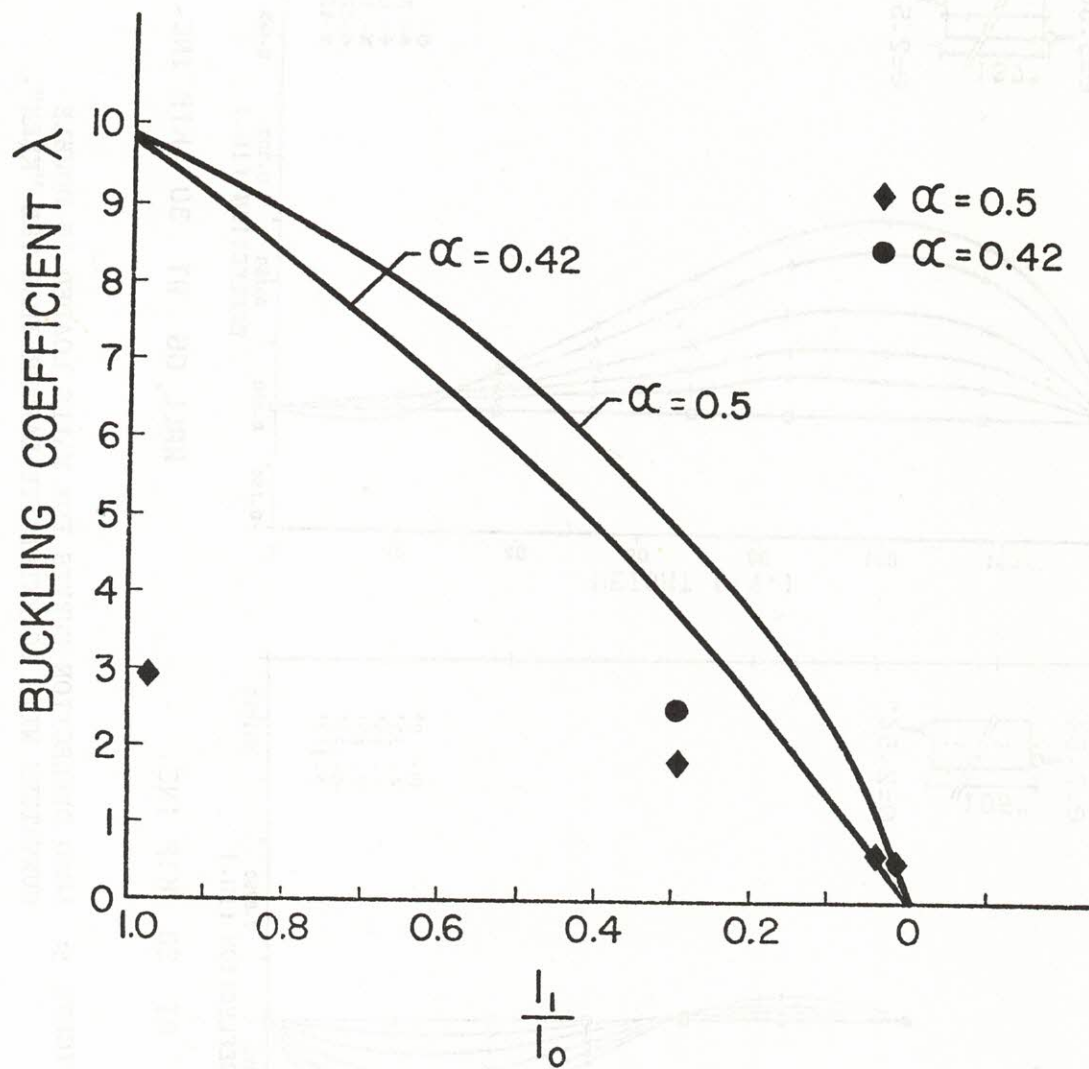


FIGURE 6. RELATION BETWEEN CALCULATED AND EXPERIMENTAL RESULTS